RSC Advances

ROYAL SOCIETY OF CHEMISTRY

www.rsc.org/advances

RSC Advances

RSCPublishing

ARTICLE

Synthesis of novel dispiropyrrolothiazoles by three-component 1,3-dipolar cycloaddition and evaluation of their antimycobacterial activity

Cite this: DOI: 10.1039/x0xx00000x

Received 00th October 2014,
Accepted 00th January 2012

DOI: 10.1039/x0xx00000x

www.rsc.org/

Saoussen Haddad,[a,b] Sarra Boudriga,[a] François Porzio,[b] Armand Soldera,[b] Moheddine Askri,[a,*] Dharmarajan Sriram,[c] Perumal Yogeeswari,[c] Michael Knorr,[d] Yoann Rousselin,[e] Marek M. Kubicki[e]

In an on-going effort to develop novel anti-tubercular agents, a series of original dispiropyrrolothiazole derivatives have been synthesized by three-component 1,3-dipolar cycloaddition of *(E)*-3-arylidene-1-phenyl-pyrrolidine-2,5-diones, 1,3-thiazolane-4-carboxylic acid and cyclic diketones. The stereochemistry of the spiranic adducts has been confirmed by an X-ray diffraction analysis. Theoretical calculations have been carried out using DFT approach at the B3LYP/6-31G(d,p) level allowing to enlighten the observed regio- and stereoselectivity. The newly synthesized compounds were screened *in vitro* against *Mycobacterium tuberculosis* H37Rv and the most active compounds were tested for cytotoxicity studies. Some compounds exhibited significant activity, in particular dispiropyrrolothiazole derivatives **15c** and **15f** emerged as the most promising antitubercular agents.

Introduction

Tuberculosis (TB), a contagious disease caused mainly by *Mycobacterium tuberculosis* (MTB), has infected 8.7 million people during 2011 and led to the death of 1.4 million people the same year as reported by the World Health Organization (WHO).[1] Moreover, it is estimated that one third of the world's population have latent *M. tuberculosis*. The spread of this disease was activated by co-infection of patients with the Human Immunodeficiency Virus (HIV).[2] The current treatment for susceptible strains prescribed under Directly Observed Treatment Short Course (DOTS) requires at least 6 months of drug therapy using a combination of four drugs that have been discovered in the last four decades.[3] However, long duration therapy, associated toxicity and emergence of multi drug-resistant tuberculosis (MDR-TB), highlight the need to explore new potent tuberculosis drugs, exhibiting novel mechanisms of action, with the aim of shortening and improving TB treatment.
Nitrogen spiro-heterocycles are important structural building blocks featured in a large number of naturally occurring alkaloids, drugs and pharmaceutically active compounds.[4] In particular, spiropyrrolothiazole derivatives are interesting for their exhibition of a wide range of biological activities such as antidiabetic,[5] anticancer,[6] antimicrobial[7] and acetylcholinesterase-inhibitory behaviour.[8] It is relevant to point out that spiropyrrolothiazole derivatives bearing oxindolyl **1-5** or acenaphthylenonyl cores **6** also exhibit antimycobacterial properties.[9] Many molecules comparable or even better activities than some of the currently employed first-line drugs, ethambutol, isoniazid and pyrazinamide or the second-line agent ciprofloxacin, for TB treatment (Fig.1).

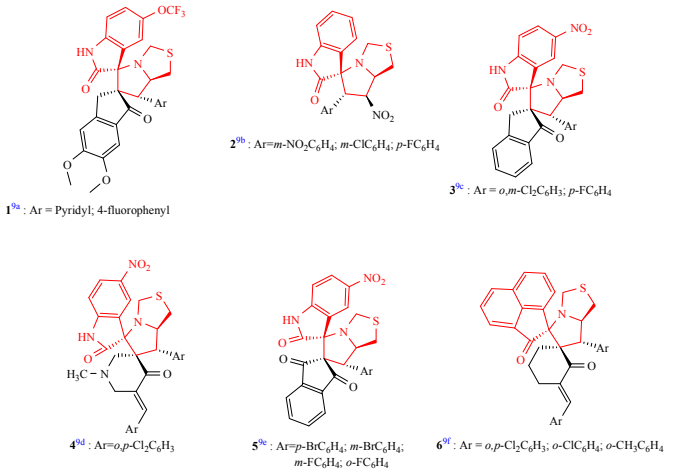

Fig.1. Representative antitubercular agents derived from spiropyrrolothiazoles **1-6**

On the other hand, the pyrrolidine-2,5-dione core is found in some alkaloids including Hirsutellone A and B **7** as well as in

synthesized compounds **8-9**, which have been recognized to display significant growth inhibitory activity against *Mycobacterium tuberculosis* H37Rv strain (Fig.2).[10]

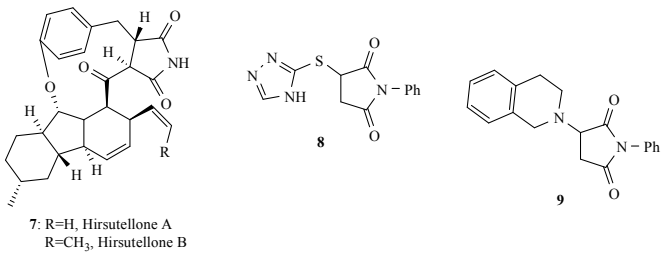

Fig 2. Examples of N-heterocyclic compounds incorporating a pyrrolidine-2,5-dione motif and exhibiting antimycobacterial activity

It thus appeared relevant to integrate both the spiropyrrolothiazole and pyrrolidine-2,5-dione motif in one molecule to generate an original scaffold for biological evaluations. The targeted molecules were efficiently synthesized through multi-component sequential reaction of (*E*)-3-arylidene-1-phenyl-pyrrolidine-2,5-diones **10**, 1,3-thiazolane-4-carboxylic acid **11** and isatin **12** or acenaphthenequinone **13** (Scheme 1). This well reported methodology has already been estabilished as a powerful tool for the construction of spiropyrrolothiazole derivatives using amino acid **11**, diketones **12** or **13** and various alkenes. The resulting structures have shown significant interest as an antitubecular precursors.[9-11]

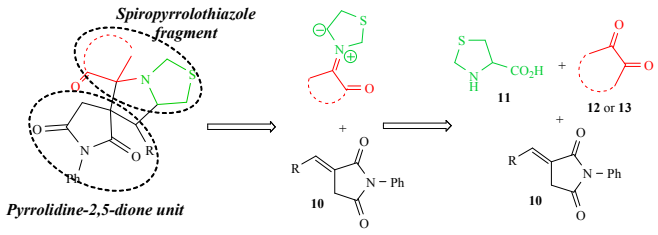

Scheme 1. Retrosynthesis strategy for synthesis the spiropyrrolothiazole-pyrrolidine-2,5-dione hybrids

Prasanna and co-workers[9c] discussed on the first example the different approach mode *endo/exo* of the possible conformations of azomethine ylide derived from isatin and thiazolidine-4-carboxylic acid toward dipolarophile.

It is worth noting that no theoretical investigation to better understand this kind of reaction have been reported yet. We thus explicitly studied the regio- and stereochemistry from a theoretical point of view by means of the Density Functional Theory (DFT).

Very encouraging activities for some of the synthesized compounds against *M. Tuberculosis* H37Rv growth are finally reported supporting our approach.

Results and discussion

Synthesis and characterization of the cycloadducts using isatins

The *(E)*-3-arylidene-1-phenyl-pyrrolidine-2,5-diones **10** used as starting materials were prepared by Wittig reaction according a protocol described in the literature.[12] The reaction of the imides **10** with non-stabilized azomethine ylides, generated *in situ* by the decarboxylative condensation of 1,3-thiazolane-4-carboxylic acid **11** with various substituted isatin (1*H*-indole-2,3-dione**)** derivatives **12** in refluxing methanol, afforded straightforwardly a large series of dispiropyrrolothiazole derivatives **14–16** in a stereoselective manner according Scheme 2. We found no spectroscopic evidence for a competing formation of isomeric compounds **14'–16'**.

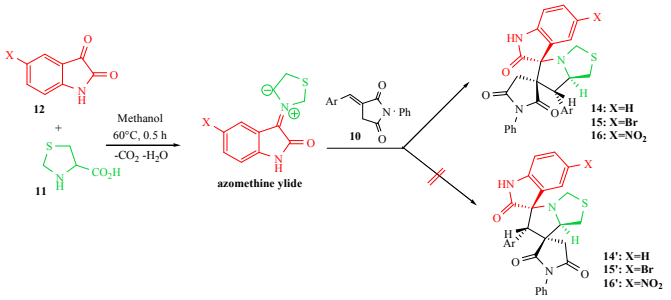

Scheme 2. Reaction of *(E)*-3-arylidene-1-phenyl-pyrrolidine-2,5-diones **10** with 1,3-thiazolane-4-carboxylic acid **11** and isatin **12**

The targeted spiroadducts **14-16** were obtained as colourless solids in very satisfying yields between 80–92% (Table 1), regardless of the electronic properties of the substituent at the *p*-position of the aryl group (H, CH_3, OCH_3, Cl, F and SCH_3) of dipolarophile **10**.

Table 1. Synthesis of dispiropyrrolothiazole derivatives **14–16**[a]

Entry	Compound	X	Ar	Yield (%)[b]
1	**14a**	H	C_6H_5	89
2	**14b**	H	*p*-MeC_6H_4	83
3	**14c**	H	*p*-$MeOC_6H_4$	86
4	**14d**	H	*p*-ClC_6H_4	91
5	**14e**	H	*p*-FC_6H_4	80
6	**14f**	H	*p*-$CH_3SC_6H_4$	83
7	**15a**	Br	C_6H_5	87
8	**15b**	Br	*p*-MeC_6H_4	91
9	**15c**	Br	*p*-$MeOC_6H_4$	83
10	**15d**	Br	*p*-ClC_6H_4	89
11	**15e**	Br	*p*-FC_6H_4	90
12	**15f**	Br	*p*-$CH_3SC_6H_4$	82
13	**16a**	NO_2	C_6H_5	80
14	**16b**	NO_2	*p*-MeC_6H_4	86
15	**16c**	NO_2	*p*-$MeOC_6H_4$	88
16	**16d**[c]	NO_2	*p*-ClC_6H_4	-
17	**16e**	NO_2	*p*-FC_6H_4	87
18	**16f**	NO_2	*p*-$CH_3SC_6H_4$	85

[a]The reactions were carried out with **10** (1 mmol), **11** (1.5 mmol) and **12** (1 mmol) in methanol (10mL) at 60°C for 0.5 h.
[b] Isolated yield after purification by column chromatography.
[c]Failure to separate

The structure of the spiroadducts was characterized by IR, ^1H NMR, ^{13}C NMR and an X-ray structure analysis, as

exemplified for cycloadduct **14a**. The IR spectrum of **14a** exhibits absorptions at 1712, 1774 and 3166 cm^{-1} due to C=O oxindole, C=O imide and N-H stretching vibrations, respectively. Selected ^{1}H and ^{13}C chemical shifts assignment of **14a** are shown in Fig.3.

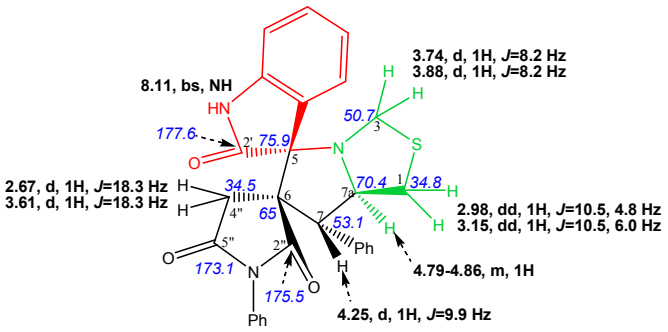

Fig.3. Selected ^{1}H and ^{13}C NMR chemical shifts of **14a**

The ^{1}H NMR spectrum of **14a** exhibits two doublets at δ 2.67 and δ 3.61 ppm (J = 18.3 Hz) corresponding to the 4″-CH_2 group. The hydrogen atoms from 1-CH_2 appear as a doublet of doublets at 2.98 (J = 10.5 and 4.8 Hz) and 3.15 ppm (J = 10.5 and 6.0 Hz). The doublets at 3.74 and 3.88 ppm (J = 8.2 Hz) are assigned to the 3-CH_2 hydrogen atoms. The H-7 and H-7a protons appear as a doublet at 4.25 ppm (J = 9.9 Hz) and a multiplet at 4.79-4.86 ppm, respectively. The multiplicity of the signals, doublet and multiplet, are clearly corroborating the regiochemistry of the cycloaddition reaction. If the hypothetical alternative regioisomer **14'a** (Scheme 2) would have been formed, the pyrrolizidinyl protons H-7 and H-7a should give rise to a singlet and doublet of doublet pattern in the ^{1}H NMR spectrum. A board singlet broad at 8.11 ppm indicates the presence of the NH proton of the oxindole ring.

The ^{13}C NMR spectrum shows two peaks at δ 65.0 and 75.9 ppm, corresponding to the two spirocarbons C-6 and C-5. The occurrence of peaks at δ 173.1, 175.5 and 177.6 ppm confirm the presence of three carbonyl groups. In the DEPT-135 spectrum, the peaks at δ 34.5, 34.8 and 50.7 ppm indicate the presence of three methylene groups. The pyrrolizidinyl carbons C-7 and C-7a appear at δ 53.1 and 70.4 ppm, respectively. The reactions were found to be highly regioselective leading to the formation of only one isomer **14a**, no indication for the presence of regioisomer **14'a** was found (Scheme 2).

The stereochemical outcome of the cycloaddition was also corroborated by an X-ray diffraction study of the crystal structure of the cycloadduct **14a**, whose ORTEP diagram is displayed in Fig. 4. The molecules of **14a** crystallize in the centro-symmetric triclinic space group P-1. Consequently, one intrinsically chiral molecule (as the one shown in Fig. 4) with C9, C11, C21 and C22 atoms in *R* chirality has an opposite isomer (enantiomer) giving rise to the overall racemic structure.

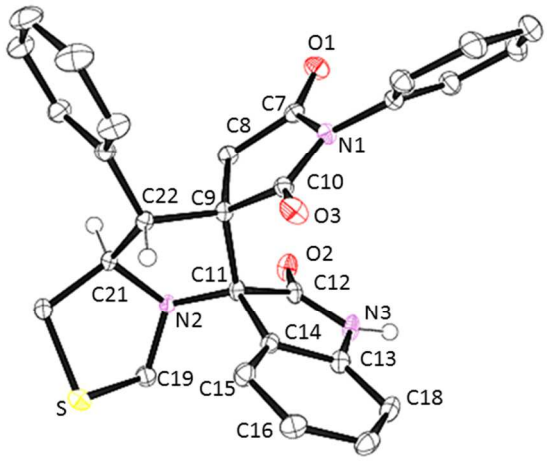

Fig. 4. ORTEP of the molecular structure of cycloadduct **14a** in the crystal at 50 % probability level (115K). For clarity, only stereo-chemically significant hydrogen atoms are shown. Selected bond lengths (Å) and angles (°): C9–C8 1.5345(16), C9-C10 1.5256(16), C9–C11 1.5799(17), C9-C22 1.5515(16), C11-N2 1.4695(15), C11-C12 1.5644(16), C11-C14 1.5318(17); C7-N1-C10 111.95(10), C19-N2-C21 111.25(10), C19-N2-C11 117.42(10), C11-N2-C21 110.45(9), C12–N3–C13 111.46(10).

The fused heterocycle formed by 9 atoms (C11, C12, N3, C13 through C18) is almost planar with the largest deviation from the best least square plane of some 0.06 Å observed for the C11 and C12 atoms. This suggests a high degree of π conjugation in this part of the molecule. The dihedral angles including both spiranic carbon atoms C9 and C11 are close to 90°: 85.66(7)° for the C11/C12/C14//N2/C11/C9 and 89.45(7)° for the C11/C9/C22//C8/C9/C10 planes. One also notes that the N1 and N3 atoms are in a perfect trigonal planar hybridization (sum of three angles around are equal to 359.8 and 360°, respectively). The N2 atom adopts a pyramidal structure with the sum of three angles between the σ bonds in order of 339.1°.

The ORTEP diagram reveals that *(i)* the two carbonyl carbons C-2″ (C-10 in ORTEP) and C-2′(C-12 in ORTEP) are in *trans*-relationship, and *(ii)* reveals a *cis*-relationship between the proton attached at C-7 (C-22 in ORTEP) and the carbonyl carbon C-2′.

Thus, the cycloadduct is formed through an *exo*-approach between the *(E)*-3-arylidene-1-phenyl-pyrrolidine-2,5-diones and *anti*-**12a** (Scheme 2). The cycloaddition proceeded *via* an *exo*-transition state affording only one diastereomer, as found in many similar cycloaddition studies.[9-11]

DFT calculations

To better understand the observed regio- and stereoselectivity, the 1,3-dipolar cycloaddition reactions of the azomethine ylide **12a** with dipolarophile **10a** has been theoretically studied using the DFT approach. Such calculations aim to unveil the reaction pathway predicted by DFT to shed light on the experimental behaviour. All the Gibbs energies that are discussed in the text have been computed within the harmonic approximation at a temperature of 298.15 K, and a pressure of 1.0 atmosphere and within the harmonic approximation. The optimized geometry of the dipole **12a** reveals its planar structure; it actually exists in

two diasteromeric *syn*- and *anti*-forms (Scheme 3). The *syn*-**12a** form is slightly more stable than the *anti*-**12a** form with a difference between their respective Gibbs energy of $\Delta G_{syn\text{-}anti}$ = 0.40 kcal.mol^{-1}. This energy difference is lower that the thermal energy at 298 K (k_B.T = 0.6 kcal.mol^{-1}). The attack of the dipolarophile on *syn*-**12a** results in an unfavourable inward movement of the 1,3-thiazolane ring towards the isatin ring, which lead to the steric hindrance between these later nucleus. While on *anti*-**12a**, it results in a favourable outward movement[13] (Scheme 3). Hence, the computational investigation is focused on the *anti*-**12a** conformation.

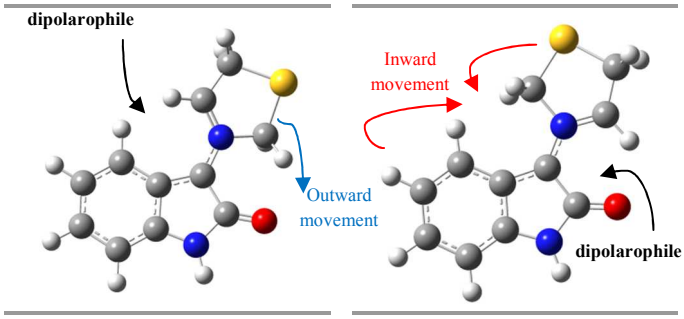

anti-**12a** $\Delta G_{syn\text{-}anti}$ = 0.40 kcal.mol^{-1}

syn-**12a** $\Delta G_{syn\text{-}anti}$ = 0 kcal.mol^{-1}

Scheme 3. Gibbs energies of *anti*- and *syn*- forms of azomethine ylide **12a** calculated at the B3LYP/6-31G (d,p) level. The mode of the attack of the dipolarophile is also represented.

A study using the frontier molecular orbital (FMO) model[14] was first carried out. This theory is based on the statement that a valuable estimate of the actual reactivity can be achieved by unveiling interaction between the HOMO and the LUMO of the reactants.[15] As shown in Fig. 5, the energy gap $HOMO_{anti\text{-}12a}$–$LUMO_{10a}$ (3.817 eV) is lower than the $LUMO_{anti\text{-}12a}$ and the $HOMO_{10a}$ (4.949 eV). This attests that the $HOMO_{dipole}$-$LUMO_{dipolarophile}$ interaction controls the cycloaddition reaction within a normal electron demand reaction.

The analysis of the global and local indices for electrophilic/nucleophilic is a powerful tool to grasp the reactivity in polar cycloadditions. In Table S1 (in the ESI), the static global properties, namely electronic chemical potential μ, chemical hardness η, and the electrophilicity index ω are reported. We can notice that μ of dipole-1,3 (-3.776 eV) is greater than μ of dipolarophile **10a** (-4,343 eV) and η of *anti*-**12a** (4.170 eV) is lower than η of **10a** (4,596 eV). Consequently, the charge transfer will take place from ylide *anti*-**12a** to dipolarophile **10a**. On the other hand, the electrophilicity values show that ω of dipolarophile **10a** (2,052 eV) is greater than ω of azomethine ylide *anti*-**12a** (1.710 eV), indicating that *anti*-**12a** will act as a nucleophile whereas **10a** will act as an electrophile.

After evaluating the global nucleophilic/electrophilic character, a local reactivity is analyzed by means of the condensed Fukui functions, the cationic and anionic systems were kept at the optimized geometries of the corresponding neutral systems. Fukui function parameters were evaluated by using the technique of electrostatic potential (ESP) derived atomic

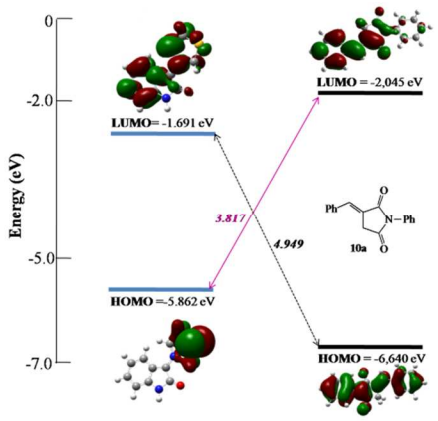

Fig.5 HOMO and LUMO energies of *anti*-**12a** and dipolarophile **10a** calculated at the B3LYP/6-31G(d,p) level

populations. The calculated local chemical reactivity parameters of *anti*-**12a** and dipolarophile **10a** are shown in Table S2 (in the ESI). In the reaction between dipolarophile **10a** and azomethine ylide *anti*-**12a**, the most favored interactions take place between the C-5" centre of *anti*-**12a** (possessing the highest value of f^- = 0.253) and the C-6 center of **10a** (possessing the highest value of f^+ = 0.154). These results are in prefect agreement with the afore-mentioned experiment (Scheme 2).

The four reactions shown in Scheme 4 were theoretically investigated. They consist of *i)* two regioisomeric channels and ii) *endo* and *exo* stereoisomeric approach modes between the *anti*-dipole **12a** and the dipolarophile **10a**. The cycloadducts were labelled *endo*-**14a**, *exo*-**14a**, *endo*-**14'a**, *exo*-**14'a** and their transition states (TS) *endo*-**TS1**, *exo*-**TS1**, *endo*-**TS2**, *exo*-**TS2** were energetically optimized and characterized under the same level of calculation by using the Berny analytical gradient method.[16] These TS, which are characterized by saddle point leading to the occurrence of one imaginary frequency, are displayed in Fig. 6.

At the TSs associated with the regioisomeric channels 1, the length of the C-3–C-3' forming bonds are 2.786 Å at *endo*-TS1 and 2.839 Å at *exo*-TS1, while the distance between the C-6 and the C-5" atoms is 2.035 Å at *endo*-**TS1** and 2.063 Å at *exo*-**TS1**. Considering the TSs associated with the regioisomeric channels 2, the length of the C-6-C-3' forming bonds are 2.536 Å at *endo*-**TS2** and 2.385 Å at *exo*-**TS2**. The extent of the asynchronicity on the bond-formation can be measured by means of the difference between the lengths of the two σ bonds that are being formed in the reaction that is, $\Delta d = d_1 - d_2$.[16] asynchronicity at the regioisomeric channels 1 is Δd = 0.750 Å at *endo*-**TS1** and 0.776 Å at *exo*-**TS1**, while that at the regioisomeric channels 2 is Δd = 0.430 Å at *endo*-**TS2** and 0.241 Å at *exo*-**TS2**. These geometrical parameters show that these cycloadditions correspond to asynchronous concerted processes. Moreover, TSs corresponding to the regioisomeric channels 1 are more advanced.

An analysis of the IRC[17] cycloaddition profile, using the Hessian based predictor-corrector (HPC) method[18] were used to

RSC Advances

RSCPublishing

ARTICLE

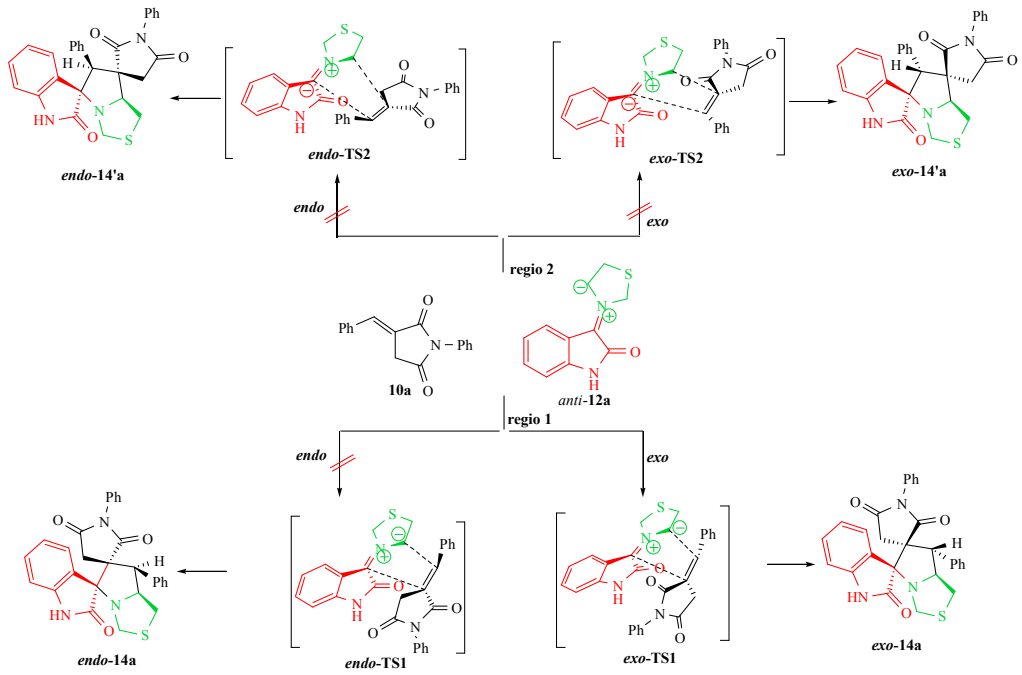

Scheme 4. Plausible mechanism for the formation of **14a**

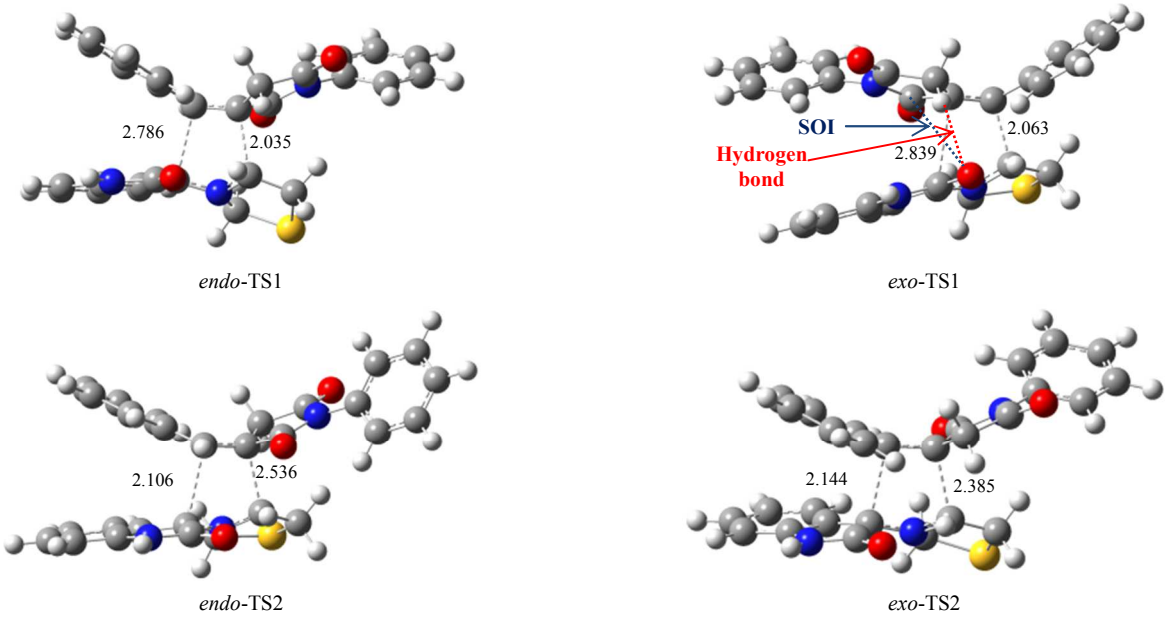

Fig.6. The four possible transition states for the 1,3-dipolar cycloaddition of *anti*-**12a** across **10a** optimized at the B3LYP/6-31G(d, p) level. The values of the lengths of the C-C bonds directly involved in the reaction are given in angstroms. Coordinates are given in the Supporting Information.

confirm that these 1,3-dipolar cycloaddition reactions take place along asynchronous concerted processes. These results are in agreement with previous studies.[19]

The Gibbs free energy (ΔG), enthalpy (ΔH) and entropy (ΔS), for the different stationary points along the reactive channels are reported in Table 2. All the energy values have been corrected for zero point energy. The kinetic parameters

(activation energy, activation enthalpies and activation entropies, between reactants and transition states) are first discussed. It is observed that the activation energy for the TSs increases in the following order: *exo*-**TS1**<*exo*-**TS2**<*endo*-**TS1**<*endo*-**TS2**. The most favourable pathway, *via* the *exo*-**TS1**, exhibits a very lower activation energy (20.3 kcal.mol^{-1}) than that stemmed from the second most probable route (26.3 kcal.mol^{-1}). The *exo*-**TS1** is thus the kinetically favourable pathway. Investigation of activation enthalpies and entropies for these cycloadditions also revealed that the *exo*-**TS1** pathway is more favourable from these two viewpoints. From an energy point of view, structural investigation (Fig. 6) of these two TS reveals that the dipole and dipolarophile are largely superimposed in the *exo*-**TS1**. Thus, the significantly lowest energy value of *exo*-**TS1** can be partially explained by secondary orbital interactions (SOI) in *exo*-**TS1**, which occurs between the oxygen atom of the carbonyl of the isatin and the carbon atom of the carbonyl of the dipolarophile. Moreover, an additional hydrogen bond takes place through in *exo*-**TS1**, between one of the methylene hydrogen atoms of dipolarophile **10a** with the carbonyl of the azomethine ylide **12a** (2.406 Å).[20] The analysis of the thermodynamic parameters (Gibbs free energy (ΔG), enthalpy (ΔH) and entropy (ΔS), between reactants and products) of the studied reactions. It is observed that the lowest ΔG values stem from the *endo* approach on **14'a.** However, the Gibbs free energy difference between the two products of lowest energies (*endo*-**14'a** and *exo*-**14a**, -1.8 and –1.4 kcal.mol^{-1}, respectively) is underneath the thermal energy value at 298.15 K (0.6 kcal mol^{-1}). Moreover, all cycloadditions are exothermic processes, and ΔH is in the range of -13.0 to -17.4 kcal.mol^{-1}. Contrary to kinetic parameters, it appeared that both entropies and enthalpies are similar among the most favorable thermodynyamics products. This evidence thus suggests that a kinetic control takes place. Accordingly, DFT investigation shows that the most favorable pathways goes through *exo*-**TS1** (*exo*-**14a**) under kinetic control. Such a conclusion is in perfect agreement with the experimental observation assigning the *exo*-regioisomer **14a** as the only formed product.

Table 2. Relative Gibbs free energies at 298.15 K (ΔG, in kcal.mol^{-1}), enthalpies (ΔH, in kcal.mol^{-1}) and entropies (ΔS, in cal.mol^{-1}.K^{-1}) for TSs and adducts of 1.3-dipolar cycloaddition between *anti*-**12a** and **10a**, calculated at the B3LYP/6-31G(d,p) level.

	ΔG	***ΔH***	***ΔS***
endo-**TS1**	28.9	14.4	-48.7
exo-**TS1**	20.3	4.9	-51.6
endo-**TS2**	30.7	16.5	-47.5
exo-**TS2**	26.3	11.3	-50.3
endo-**14a**	3.0	-13.0	-53.9
exo-**14a**	-1.4	-17.4	-53.4
endo-**14'a**	-1.8	-17.3	-52.1
exo-**14'a**	-0.7	-16.6	-53.2

Synthesis and characterization of the cycloadducts using acenaphthenequinone

To investigate further the regio- and stereoselectivity of the cycloaddition, we carried out the three-component 1,3-dipolar cycloaddition reaction of the dipolarophile **10** with another azomethine ylide generated *in situ* from 1,3-thiazolane-4-carboxylic acid **11** and acenaphthenequinone **13** as diketones. Under similar reaction conditions, this reaction afforded the corresponding dispiropyrrolothiazole derivatives **17a–e** in good yields (82–90%) as shown in Scheme 5 and Table 3.

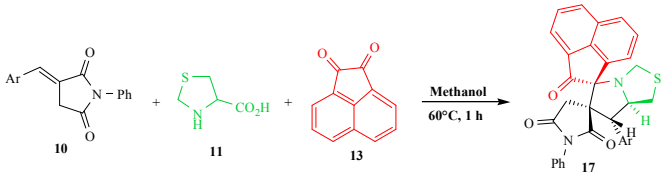

Scheme 5. Reaction of *(E)*-3-arylidene-1-phenyl-pyrrolidine-2,5-diones **10** with 1,3-thiazolane-4-carboxylic acid **11** and acenaphtenequinone **13**

Table 3. Synthesis of dispiropyrrolothiazole derivatives **17**[a]

Entry	Compound	Ar	Yield (%)[b]
1	**17a**	C_6H_5	87
2	**17b**	*p*-MeC_6H_4	88
3	**17c**	*p*-$MeOC_6H_4$	90
4	**17d**	*p*-ClC_6H_4	80
5	**17e**	*p*-FC_6H_4	82

[a] The reaction was carried out with **10** (1 mmol), **11** (1.5 mmol) and **13** (1 mmol) in methanol (10 mL) at 60°C for 1h.
[b] Isolated yield after purification by column chromatography

The structural and stereochemical features of all derivatives in series **17** are fully supported by the IR and NMR spectroscopic data. As illustrated for compound **17b**, two intense IR absorption bands at 1709 and 1791 cm^{-1}, are observed in the IR spectrum. They correspond to the acenaphtenone and imide ring carbonyls, respectively. The ^{1}H and ^{13}C spectroscopic data of **17b** are summarized in Fig. 7.

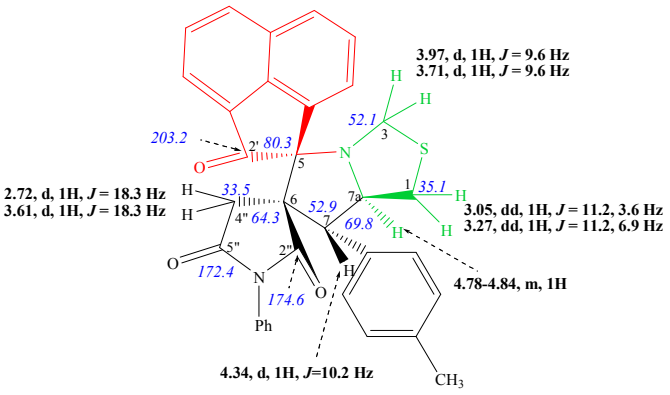

Fig. 7. Selected 1H and 13C NMR chemical shifts of **17b**

The ^{1}H NMR spectrum of **17b** displays a doublet at δ 4.34 ppm (J = 10.2 Hz) and a multiplet between 4.78-4.84 ppm, corresponding to the H-7 and H-7a protons, respectively. These data confirm the regiochemistry of the cycloaddition reaction. The signals at 64.3 ppm and 80.3 ppm in the ^{13}C NMR spectrum of **17b** are attributed to the presence of two spiro-carbons C-6 and C-5, respectively. The resonance at 203.2 ppm

is characteristic of the presence of the carbonyl group from the acenaphthenequinone moiety.

Biological activities

In-vitro MTB screening

All new compounds were screened for their *in vitro* anti-mycobacterial activity against *M. tuberculosis* H37Rv using the agar dilution method[21] and drug concentrations from 50 µg/mL to 0.78 µg/mL. The MIC is defined as the minimum concentration of compound required to achieve complete inhibition of bacterial growth. This method agrees with the procedure recommended by the National Committee for Clinical Laboratory Standards for the determination of MIC in triplilicate. The MIC's of the synthesized compounds **14-17** are reported in Table 4 along with the MIC's of several standard drugs for comparison.

Table 4. Antimycobacterial activities of dispiropyrrolothiazole derivatives **14-17**

Entry	Comp.	X	Ar	MTB[a] (MIC) µg/mL	Cytotoxicity (RAW 264.7 cells) % inhibition
1	**14a**	H	C_6H_5	3.125	32.4
2	**14b**	H	*p*-MeC_6H_4	25	*ND*
3	**14c**	H	*p*-$MeOC_6H_4$	3.125	28.63
4	**14d**	H	*p*-ClC_6H_4	25	*ND*
5	**14e**	H	*p*-FC_6H_4	25	*ND*
6	**14f**	H	*p*-$CH_3SC_6H_4$	50	*ND*
7	**15a**	Br	C_6H_5	*NT*	*NT*
8	**15b**	Br	*p*-MeC_6H_4	50	*ND*
9	**15c**	Br	*p*-$MeOC_6H_4$	1.56	27.63
10	**15d**	Br	*p*-ClC_6H_4	6.25	30.16
11	**15e**	Br	*p*-FC_6H_4	12.5	*ND*
12	**15f**	Br	*p*-$CH_3SC_6H_4$	1.56	20.74
13	**16a**	NO_2	C_6H_5	*NT*	*NT*
14	**16b**	NO_2	*p*-MeC_6H_4	6.25	28.15
15	**16c**	NO_2	*p*-$MeOC_6H_4$	12.5	*ND*
16	**16d**	NO_2	*p*-ClC_6H_4	*NT*	*NT*
17	**16e**	NO_2	*p*-FC_6H_4	25	*ND*
18	**16f**	NO_2	*p*-$CH_3SC_6H_4$	50	*ND*
19	**17a**	H	C_6H_5	3.125	35.62
20	**17b**	H	*p*-MeC_6H_4	50	*ND*
21	**17c**	H	*p*-$MeOC_6H_4$	3.125	43.12
22	**17d**	H	*p*-ClC_6H_4	25	*ND*
23	**17e**	H	*p*-FC_6H_4	25	*ND*
Isoniazid				0.05	
Rifampicin				0.1	
Ciprofloxacin				3.13	
Ethambutol				1.56	
Pyrazinamide				6.25	

[a]Mycobacterium tuberculosis H37Rv. *NT*: not tested. *ND*: not determined.

The spiroheterocycles **14-17** have MICs in the range of 1.56–50 µg/mL (Table 3). Among them, eight compounds (**14a**, **14c**, **15c**, **15d**, **15f**, **16b**, **17a** and **17c**) were found to be more or equally active against MTB than the first line anti-TB drug pyrazinamide (MIC 6.25µg/mL), whilst six of them **14a**, **14c**, **15c**, **15f**, **17a** and **17c** were more potent than ciprofloxacin (MIC 3.13µg/mL). All compounds are however less potent than rifampicin and isoniazid. The dispiropyrrolothiazole derivatives **15c** and **15f** displayed the maximum potency with MICs of 1.56 µg/mL, thus being equipotent with ethambutol. Noteworthy is the fact that the latter two heterocycles are two and four times more potent than the standard drugs ciprofloxacin and pyrazinamide, respectively.

The influence of the substituents at the isatin core as well as on the aryl rings was examined for structure–activity relationship (SAR). As shown in Table 3, the substituent present on the isatin nucleus has a very strong effect on the activity of spiropyrrolothiazole derivatives **14-16**. The order of activity, in general, being Br>H>NO_2 was evidenced from the observation that three compounds in series **15** (**15c**, **15d** and **15f**), two in series **14** (**14a** and **14c**), and one in series **16** (**16b**) were more active against MTB (Table 3).

In-vitro cytotoxicity screening

Some of the selected compounds were also tested for *in vitro* cytotoxicity against RAW 264.7 cells at 50 µM concentration using a (4,5-dimethylthiazol-2-yl)-2,5-diphenyltetrazolium bromide (MTT) assay. The percentage of cells inhibition is reported in Table 3. The most promising anti-TB compounds **15c** and **15f** showed 27.63 and 20.74 % inhibition, respectively, at 50 µM.

Conclusions

In this study we demonstrated that the literature-known three-component 1,3-dipolar cycloaddition of azomethine ylides generated in situ can also be applied to the synthesis of a series of novel dispiropyrrolothiazole derivatives with isatin or acenaphtenequinone using arylidene-succinimide as alkene component. This reaction can be conducted under convenient and mild reaction conditions, affording efficiently the cycloaddition products with high yields in a complete regio- and stereoselective manner.

An analysis based on theoretical calculations using the DFT approach, B3LYP/6-31G(d,p) showed that the spirocycloadduct **14** is obtained through a 1,3-dipolar cycloaddition reaction via a high asynchronous mechanism with a very low activation energy, as compared to the three other possible reaction paths. This outcome is in agreement with the experimental observations.

Screening all these derivatives against Mycobacterium tuberculosis H37Rv and cytotoxicity revealed that **15c** and **15f** are the most active antitubercular agents compared to the other evaluated compounds.

Experimental

General information and apparatus

NMR spectra were recorded with a Bruker-Spectrospin AC 300 spectrometer operating at 300 MHz for ^{1}H and 75 MHz for ^{13}C using tetramethylsilane (TMS) as internal standard (0.00 ppm) in $CDCl_3$ as solvent. The following abbreviations were used to explain the multiplicities: bs = broad singlet, s = singlet, d = doublet, dd = doublet of doublets, m = multiplet. IR spectra were recorded on a Perkin-Elmer Spectrum Two™ FT-IR in the ATR mode. Elemental analyses were performed on a Perkin Elmer 2400 Series II Elemental CHNS analyzer. Materials: thin-layer chromatography (TLC): TLC plates (Merck, silica gel 60 F_{254} 0.2 mm 200×200 nm); substances were detected using UV light at 254 nm.

General procedure for the preparation of cycloadducts 14-17

A mixture of **10** (1.0 mmol), 1,3-thiazolane-4-carboxylic acid **11** (1.5 mmol) and isatin **12** or acenaphthenequinone **13** was refluxed in methanol (10 mL) for 0.5-1h. After completion of the reaction as monitored from TLC, the mixture was poured into ice-water (50 mL). The resulting solid was filtered off and purified by flash column chromatography on silica gel employing ethylacetate-cyclohexane (3:7 v/v) as eluent to obtain the pure products **14-17**. Spectroscopic data for the all compound are presented in the ESI.

DFT calculations

All calculations have been performed using the Gaussian 09 package.[22] The hybrid density functional theory B3LYP[23] with the 6-31G(d,p) basis set[24] was employed to compute the energy. The optimization procedure was carried out using the Berny analytical gradient method.[16] The stationary points were characterized through frequency calculations in order to ensure that the minima in energy, i.e. reactants and products, as well as transition states (TS) exhibit zero and one imaginary frequency, respectively. Intrinsic reaction coordinate (IRC)[17] calculations starting at the saddle points were carried out to check the connections between the TS, reactants and cycloadducts, using the Hessian based predictor-corrector (HPC) method.[18]

X-Ray structure study.

A colourless single-crystal of **14a** has been mounted on a Nonius Kappa Apex II diffractometer and the intensity data have been collected at 115 K using MoKα radiation of λ(Mo-Kα)= 0.71073 Å. These data were further treated with the SAINT V8.27B program suite (Bruker AXS Inc., 2012) within the OLEX2 frame.[25] The model of the structure has been solved by direct methods with SHELXS-97 and refined with SHELXL-97.[26]

Crystal and refinement data for **14a**: $C_{28}H_{23}N_3O_3S$; M = 481.55; crystal system triclinic; space group P-1, a = 9.1367(9) Å, b = 10.0617(10) Å, c = 14.3025(15) Å, α = 94.058(4), β = 99.914(4), γ = 114.73(4)°, V = 1160.7(2) $Å^3$, Z = 2, λ(Mo-Kα) = 0.71073 Å, F(000) = 504, μ(Mo-Kα) = 0.082 mm^{-1}, T = 115(2) K. 44058 reflections collected, 5333 unique and 4569 with I>2σ(I). Final agreement factors: R_1 = 0.0418 (all observed) and 0.0336 with I>2σ(I), wR_2 = 0.0888 (all observed) and 0.0832 with I>2σ(I). GOF = 1.015. Final residuals ρ_{max} = 0.371, ρ_{min} = -0.304 $e^-/Å^3$.

Crystallographic data (excluding structure factors) for the structure of **14a** have been deposited at CCDC with deposition number 990193. These data may be obtained free of charge from CCDC through www.ccdc.cam.ac.uk/data_request/cif.

Biological evaluation

In vitro MTB screening

Two-fold serial dilutions of each test compound/drug were prepared and incorporated into Middle-brook 7H11 agar medium with oleic acid, albumin, dextrose, and catalase (OADC) growth supplement to get final concentrations of 50, 25, 12.5, 6.25, 3.13, 1.56, and 0.78 μg/mL. Inoculum of M. tuberculosis H37Rv ATCC 27294 was prepared from fresh Middlebrook 7H11 agar slants with OADC (Difco) growth supplement adjusted to 1 mg/ mL (wet weight) in Tween 80 (0.05%) saline diluted to 10^{-2} to give a concentration of ~10^7cfu/mL. Five microliters of this bacterial suspension was spotted onto 7H11 agar tubes containing different concentrations of the drug as discussed above. The tubes were incubated at 37 °C, and final readings (as MIC in μg/mL) were determined after 28 days. The MIC is defined as the minimum concentration of compound required to give complete inhibition of bacterial growth. This method is similar to that recommended by the National Committee for Clinical Laboratory Standards for the determination of MIC in triplicate.

In vitro cytotoxicity screening

Antitubercular active compounds with MIC≤12.5 μg/mL were examined for toxicity in a HEK-293T cellline at the concentration of 50 μg/mL. After 72h of exposure, viability was assessed on the basis of cellular conversion of (4,5-dimethylthiazol-2-yl)-2,5-diphenyltetrazolium bromide (MTT) into a formazan product using the Promega Cell Titer 96 non-radioactive cell proliferation assay.

Acknowledgements

Computations have been made available thanks to the Calcul Quebec, and Compute Canada.

Notes and references

[a] Laboratory of Heterocyclic Chemistry Natural Products and Reactivity/LCHPNR, Department of Chemistry, Faculty of Science of Monastir, 5000 Monastir, Tunisia. E-mail: moheddine.askri@fsm.rnu.tn; Tel: +216 98676187

[b] Department of Chemistry, Quebec Center for Functional Materials, University of Sherbrooke, Sherbrooke, Québec, Canada, J1K 2R1

[c] Medicinal Chemistry and Antimycobacterial Research Laboratory, Pharmacy Group, Birla Institute of Technology & Science-Pilani, Hyderabad Campus, Jawahar Nagar, Hyderabad 500 078, Andhra Pradesh, India

[d] Institute UTINAM - UMR CNRS 6213, University of Franche-Comté, 16 Route de Gray, F-25030 Besançon, France
[e] Institute of Molecular Chemistry - UMR CNRS 6302, University of Bourgogne, 9 Avenue A. Savary, F-21078 Dijon, France
† Electronic Supplementary Information (ESI) available: [details of any supplementary information available should be included here]. See DOI: 10.1039/b000000x/

1 World Health Organization. Global tuberculosis report 2012 (in IRIS), World Health Organization, Geneva.
2 H. Mc Shane, *Int. J. STD AIDS*, 2005, **16**, 95.
3 (a) M. D. Scott, *Biochem. Pharmacol,* 2006, **71**, 1096; (b) D. J. Payne, M. N. Gwynn, D. J. Holmes and D. L. Pompliano, *Nat. Rev. Drug Discovery,* 2007, **6**, 29; (c) L. P. Ormerod, *Thorax,* 1999, **54**, 42.
4 (a) K. Arya, P. Tomarand and J. Singh, *RSC Adv.*, 2014, **4**, 3060; (b) C. E. P. Galvis and V. V. Kouznetsov, *Org. Biomol. Chem.,* 2013, **11**, 7372; (c) A. Dandia, A. K. Jainand and A. K. Laxkar, *RSC Adv.,* 2013, **3**, 8422; (d) N. R. Ball-Jones, J. J. Badillo and A. K. Franz, *Org. Biomol. Chem.,* 2012, **10**, 5165; (e) N. Hara, S. Nakamura, M. Sano, R. Tamura, Y. Funahashi and N. Shibata, *Chem. Eur. J.,* 2012, **18**, 9276; (f) N. V. Hanhan, Y. C. Tang, N. T. Tran and A. K. Frank, *Org. Lett.*, 2012, **14**, 2218; (g) K. Ohmatsu, M. Kiyokawa and T. Ooi, *J. Am. Chem. Soc.,* 2011, **133**, 1307; (h) S. W. Duan, J. An, J. R. Chen and W. J. Xiao, *Org. Lett.,* 2011, **13**, 2290; (i) B. Tan, N. Candeias and C. F. Barbas III. *Nat. Chem.*, 2011, **3**, 473; (j) K. Shen, X. Liu, G. Wang, L. Lin and X. Feng, *Angew. Chem. Int. Ed.,* 2011, **50**, 4684; (k) G. S. Singhand and Z. Y. Desta, *Chem. Rev.,* 2012, **112**, 6104; (l) M. Bandini and A. Eichholzer, *Angew. Chem, Int. Ed.,* 2009, **48**, 9608.
5 K. Atul, M. R. Awatar, S. A. Kumar, S. A. Bahadur and T. A. Kumar, *Ind. Pat. Appl*., 2011, **48**, 20110114.
6 A. Kumar, G. Gupta, S. Srivastava, A. K. Bishnoi, R. Saxena, R. Kant, R. S. Khanna, P. R. Maulikand and A. Dwivedi, *RSC Adv.,* 2013, **3**, 4731.
7 G. Wu, L. Ouyang, J. Liu, S. Zeng, W. Huang, B. Han, F. Wu, G. He and M. Xiang*, Mol. Divers.,* 2013, **17**, 271.
8 S. Sivakumar, R. R. Kumar, M. A. Ali and T. S. Choon, *Eur. J. Med. Chem*., 2013, **65**, 240.
9 (a) A. I. Almansour, S. Ali, M. A. Ali, R. Ismail, T. S. Choon, V. Sellappan, K. k. Elumalai and S. Pandian, *Bioorg. Med. Chem. Lett*., 2012, **22**, 7418; (b) S. M. Rajesh, S. Perumal, J. C. Menendez, P. Yogeeswari and D. Sriram, *Med. Chem. Commun.,* 2011, **2**, 626; (c) P. Prasanna, K. Balamurugan, S. Perumal, P. Yogeeswari and D. Sriram, *Eur. J. Med. Chem.,* 2010, **45**, 5653; (d) S. V. Karthikeyan, B. D. Bala, V. P. A. Raja, S. Perumal, P. Yogeeswari and D. Sriram, *Bioorg. Med. Chem. Lett.,* 2010, **20**, 350; (e) S. U. Maheswari, K. Balamurugan, S. Perumal, P. Yogeeswari and D. Sriram, *Bioorg. Med. Chem. Lett.,* 2010, **20**, 7278; (f) R. Kumar, S. Perumal, S. C. Manju, P. Bhatt, P. Yogeeswari and D. Sriram, *Bioorg. Med. Chem. Lett.,* 2009, **16**, 3461.
10 (a) M. Isaka, N. Rugseree, P. Maithip, P. Kongsaeree, S. Prabpai and Y. Thebtaranonth, *Tetrahedron,* 2005, **61**, 5577; (b) T. Matviiuk, G. Morid, C. Lherbeta, F. Rodriguez, M. R. Pasca, M. Gorichko, B. Guidettia, Z. Voitenko and M. Baltasa, *Eur. J .Med .Chem.,* 2014, **71**, 46.
11 (a) K. Revathy and A. Lalitha, *RSC Adv.,* 2014, **4**, 279; (b) A. A. Shvets, Yu. V. Nelyubina, K. A. Lyssenko and S. V. Kurbatov, *Russ. Chem. Bull. Int. Ed.,* 2012, **61**, 1659.
12 L. Yan, W. Yang, L. Li, Y. Shen and Z. Jiang, *Chin. J. Chem.,* 2011, **29**, 1906.
13 (a) K. Arora, S. Verma, D. Jose, P. Pardasani, and R.T. Pardasani, *Phosphorus, Sulfur, Silicon,* 2008, **183**, 1168; (b) R. T. Pardasani, P. Pardasani, A. Jain and K. Arora, *Indian J. Chem.,* 2006, **45B**, 1204.
14 K. N. Houk, *Acc. Chem. Res*., 1975, **8**, 361.
15 (a) K. Fukui, *Acc. Chem. Res*., 1981, **14**, 363; (b) K. Fukui, *Acc. Chem. Res.,* 1971, **4**, 57; (c) K. Fukui, in *Molecular Orbitals in Chemistry, Physics, and Biology; Academic*: New York, NY, 1964, pp. 525.
16 (a) M. Cossi, V. Barone, R. Cammi and J. Tomasi. *J. Chem. Phys. Lett.,*1996, **255**, 327; (b) E. Cances, B. Mennucci and J. Tomasi, *J. Chem. Phys.,* 1997, **107**, 3032; (c) V. Barone, M. Cossi and J. Tomasi, *J. Comput. Chem.,* 1998, **19**, 404.
17 K. Fukui, *J. Phys. Chem.* 1970, **74**, 4161.
18 H. P. Hratchian and H. B. Schlegel, *J. Chem. Theory and Comput.,* 2005, **1**, 61.
19 (a) C. D. Valentin, M. Freccero, R. Gandolfi and A. Rastelli, *J. Org. Chem.,* 2000, **65**, 6112-6120; (b) K. N. Houk, J. Gonzalez and Y. Li, *Acc. Chem. Res.,*1995, **28**, 81.
20 K. Chandraprakash, M. Sankaran, C. Uvarani, R. Shankar, A. Ata, F. Dallemer and P. S. Mohan, *Tetrahedron Lett.,* 2013, **54**, 3896; (b) P. Yuvaraj and B. S. R. Reddy, *Tetrahedron Lett.,* 2013, **54**, 821.
21 M. Mujahid, R.G. Gonnade, P. Yogeeswari, D. Sriram and M. Muthukrishnan, *Bioorg. Med. Chem. Lett.,* 2013, **23**, 1416.
22 M. J Frisch, G. W. Trucks, H. B. Schlegel, G. E. Scuseria, M. A. Robb, J. R. Cheeseman, G. Scalmani, V. Barone, B. Mennucci, G. A. Petersson, H. Nakatsuji, M. Caricato, X. Li, H. P. Hratchian, A. F. Izmaylov, J. Bloino, G. Zheng, J. L. Sonnenberg, M. Hada, M. Ehara, K. Toyota, R. Fukuda, J. Hasegawa, M. Ishida, T. Nakajima, Y. Honda, O. Kitao, H. Nakai, T. Vreven, J. A. Jr. Montgomery, J. E. Peralta, F. Ogliaro, M. Bearpark, J. J Heyd, E. Brothers, K. N. Kudin, V. N. Staroverov, R. Kobayashi, J. Normand, K. Raghavachari, A. Rendell, J. C. Burant, S. S. Iyengar, J. Tomasi, M. Cossi, N. Rega, N. J. Millam, M. Klene, J. E. Knox, J. B. Cross, V. Bakken, C. Adamo, J. Jaramillo, R. Gomperts, R. E. Stratmann, O. Yazyev, A. J. Austin, R. Cammi, C. Pomelli, J. W. Ochterski, R. L. Martin, K. Morokuma, V. G. Zakrzewski, G. A. Voth, P. Salvador, J. J. Dannenberg, S. Dapprich, A. D. Daniels, O. Farkas, J. B. Foresman, J. V. Ortiz and J. Cioslowski, D. J. Fox, Gaussian 09, Revision A.1; Gaussian: Wallingford CT.
23 (a) A. D. Becke, *J. Chem. Phys.,* 1993, **98**, 5648; (b) C. Lee, W. Yang and R. G. Parr, *Phys. Rev. B.*, 1998, **37**, 785; (c) B. Miehlich, A. Savin, H. Stoll and H. Preuss, *Chem. Phys. Lett.,* 1989, **157**, 200.
24 (a) R. Ditchfield, W. J. Hehre and J. A. Pople, *J. Chem. Phys.,* 1971, **54**, 724; (b) W. J. Hehre, R. Ditchfield, J. A. Pople and

J. Chem. Phys., 1972, **56**, 2257; (c) P. C. Hariharan and J. A. Pople, *Mol. Phys*., 1974, **27**, 209; (d) M. S. Gordon, *Chem. Phys. Lett.,* 1980, **76**, 163; (e) M. M. Franci, W. J. Pietro, W. J. Hehre, J. S. Binkley, D. J. De Frees, J. A. Pople and M. S. Gordon, *J. Chem. Phys.,* 1982, **77**, 3654; (f) V. A. Rassolow, J. A. Pople, M. A. Ratner and T. L. Windus, *J. Chem. Phys.,* 1998, **109**, 1223.

25 OLEX2: a complete structure solution, refinement and analysis program. O. V. Dolomanov, L. J. Bourhis, R. J. Gildea, J. A. K. Howard and H. Puschmann, *J. Appl. Cryst.,* 2009, **42**, 339.

26 G.M. Sheldrick, *Acta. Cryst.,* 2008, **A64**, 112.

A series of dispiropyrrolothiazoles derivatives has been synthesized screened *in vitro* against *Mycobacterium tuberculosis* H37Rv. The observed regio- and stereoselectivity of the cycloaddition reaction has been rationalized by DFT calculations.